Biochemical Pharmacology 225 (2024) 116299

Contents lists available at ScienceDirect

Biochemical Pharmacology

journal homepage: www.elsevier.com/locate/biochempharm

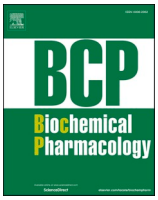

Time-dependent ligand-receptor binding kinetics and functionality in a heterodimeric receptor model

Antonio J. Ortiz [a,b,c], Víctor Martín [a,d], David Romero [f], Antoni Guillamon [d,e,f,*], Jesús Giraldo [a,b,c,**]

[a] Laboratory of Molecular Neuropharmacology and Bioinformatics, Unitat de Bioestadística and Institut de Neurociències, Universitat Autònoma de Barcelona, 08193 Bellaterra, Spain
[b] Instituto de Salud Carlos III, Centro de Investigación Biomédica en Red de Salud Mental, CIBERSAM, Spain
[c] Unitat de Neurociència Traslacional, Parc Taulí Hospital Universitari, Institut d'Investigació i Innovació Parc Taulí (I3PT), Institut de Neurociències, Universitat Autònoma de Barcelona, Spain
[d] Departament de Matemàtiques, EPSEB, Universitat Politècnica de Catalunya, 08028 Barcelona, Spain
[e] IMTech, Universitat Politècnica de Catalunya, 08028 Barcelona, Spain
[f] Centre de Recerca Matemàtica, Universitat Autònoma de Barcelona, 08193 Bellaterra, Spain

ARTICLE INFO

Keywords:
Binding kinetics
Receptor heterodimerization
Drug combination therapy
Mathematical modeling
Dynamical systems

ABSTRACT

GPCRs heteromerize both in CNS and non-CNS regions. The cell uses receptor heteromerization to modulate receptor functionality and to provide fine tuning of receptor signaling. In order for pharmacologists to explore these mechanisms for therapeutic purposes, quantitative receptor models are needed. We have developed a time-dependent model of the binding kinetics and functionality of a preformed heterodimeric receptor involving two drugs. Two cases were considered: both or only one of the drugs are in excess with respect to the total concentration of the receptor. The latter case can be applied to those situations in which a drug causes unwanted side effects that need to be reduced by decreasing its concentration. The required efficacy can be maintained by the allosteric effects mutually exerted by the two drugs in the two-drug combination system. We discuss this concept assuming that the drug causing unwanted side effects is an opioid and that analgesia is the therapeutic effect. As additional points, allosteric modulation by endogenous compounds and synthetic bivalent ligands was included in the study. Receptor heteromerization offers a mechanistic understanding and quantification of the pharmacological effects elicited by combinations of two drugs at different doses and with different efficacies and cooperativity effects, thus providing a conceptual framework for drug combination therapy.

1. Introduction

There is experimental evidence showing the existence of heterodimeric Class A GPCRs both in CNS and non-CNS regions [15]. Yet, because of the weak protein–protein interactions present in Class A heteromers, the existence of these oligomeric complexes is not an unquestionable event and needs experimental verification. In this regard, three criteria have been proposed to assess the existence of these complexes: 1. Heteromers should exhibit appropriate colocalization and interaction to enable allosterism. 2. Heteromers should exhibit distinct properties. 3. Heteromer-selective reagents should alter heteromer properties [15].

In contrast to Class A, the existence of heterodimeric Class C GPCRs offers no doubt because the union between the two subunits is made by means of a covalent bond. Importantly, the existence of metabotropic glutamate mGlu2–mGlu4 heterodimers in different brain regions has

Abbreviations: CB1, cannabinoid receptor type 1; CNS, central nervous system; GPCR, G protein-coupled receptor; ODE, ordinary differential equation; MOP, μ-opioid receptor; DOP, δ-opioid receptor; mGlu5, metabotropic glutamate receptor subtype 5; mGlu2, metabotropic glutamate receptor subtype 2; 5HT2AR, 5-hydroxytryptamine (serotonin) 2A receptor.

* Corresponding author at: Departament de Matemàtiques, EPSEB, Universitat Politècnica de Catalunya, 08028 Barcelona, Spain.
** Corresponding author at: Laboratory of Molecular Neuropharmacology and Bioinformatics, Unitat de Bioestadística and Institut de Neurociències, Universitat Autònoma de Barcelona, 08193 Bellaterra, Spain.
E-mail addresses: AntonioJesus.Ortiz@uab.cat (A.J. Ortiz), victor.martin.ortega@estudiantat.upc.edu (V. Martín), dromero@crm.cat (D. Romero), antoni.guillamon@upc.edu (A. Guillamon), Jesus.Giraldo@uab.es (J. Giraldo).

https://doi.org/10.1016/j.bcp.2024.116299
Received 13 January 2024; Received in revised form 5 May 2024; Accepted 16 May 2024
Available online 18 May 2024

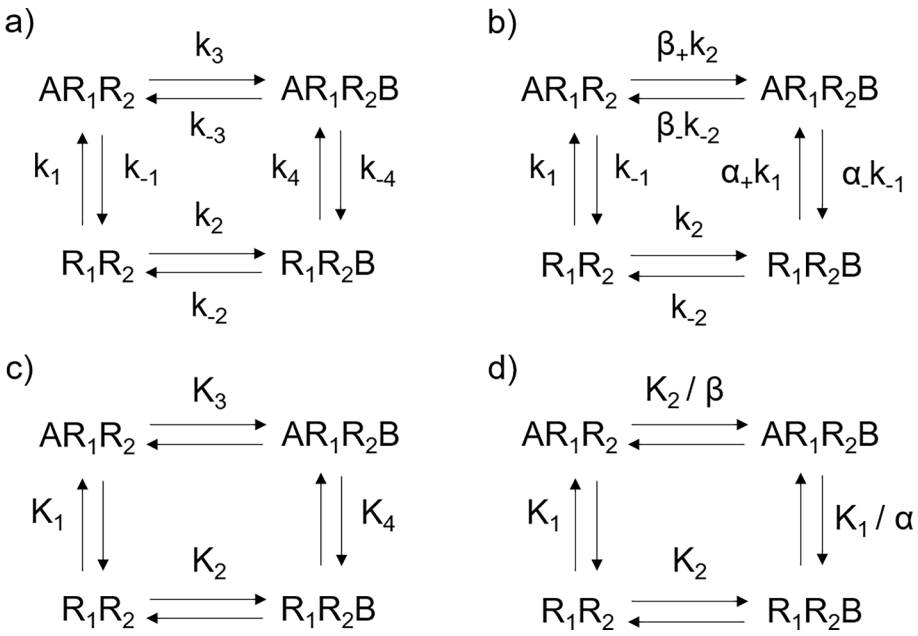

Fig. 1. Binding kinetics model of a heterodimeric receptor. Ligands A and B bind specifically to their receptor protomers, R_1 and R_2, respectively. There are four receptor species: the unbound heterodimer, R_1R_2; the singly-bound heterodimers, AR_1R_2 and R_1R_2B; and the doubly-bound heterodimer, AR_1R_2B [40]. a) Association (k_1 to k_4) and dissociation (k_{-1} to k_{-4}) rate constants are used. b) Cooperativity rate constant parameters α_+, α_-, β_+ and β_-, where $\alpha_+ = k_4/k_1$, $\alpha_- = k_{-4}/k_{-1}$, $\beta_+ = k_3/k_2$, and $\beta_- = k_{-3}/k_{-2}$, are included. It can be shown that, at equilibrium, 7 out of the 8 parameters are independent since the condition $(k_{-1}\, k_4)/(k_1\, k_{-4}) = (k_{-2}\, k_3)/(k_2\, k_{-3})$ or, equivalently, $\alpha_+/\alpha_- = \beta_+/\beta_-$, is satisfied [7]. c) Equilibrium dissociation constants (K_1 to K_4, where $K_1 = k_{-1}/k_1 = [A]_{eq}[R_1R_2]_{eq}/[AR_1R_2]_{eq}$, $K_2 = k_{-2}/k_2 = [B]_{eq}[R_1R_2]_{eq}/[R_1R_2B]_{eq}$, $K_3 = k_{-3}/k_3 = [B]_{eq}[AR_1R_2]_{eq}/[AR_1R_2B]_{eq}$, and $K_4 = k_{-4}/k_4 = [A]_{eq}[R_1R_2B]_{eq}/[AR_1R_2B]_{eq}$, are used. d) Binding cooperativity parameters α and β, where $\alpha = K_1/K_4 = \alpha_+/\alpha_- = \beta = K_2/K_3 = \beta_+/\beta_-$, are used.

been proved and quantified by using nanobody-based optical sensors [28]. Interestingly, data indicated that there are more mGlu2–mGlu4 heterodimers than mGlu4 homodimers in most regions outside the cerebellum [28]. This suggests that mGlu2-mGlu4 heteromerization is not a chance event but a consequence of biological conditions that may be a general property of mGlu heteromerization [25,29] and other Class C GPCRs, say $GABA_B$ receptors [12] and sweet and umami taste receptors [39].

It can be speculated that if there is a biological role for heteromerization of Class C GPCRs, the same must be true for heteromerization of Class A GPCRs and for heteromerization between Class C and Class A GPCRs. This leads to the conclusion that GPCR heteromerization is key in GPCR signaling (see [3,5,17,34] for more information).

GPCR heteromerization provides fine-tuning of receptor signaling. This is done by (i) activating a novel pathway different from each protomer's signaling cascade; (ii) *trans*-antagonism: activation of one receptor inhibits the signaling activity of the other; and (iii) *trans*-activation: the ability to initiate the signaling cascade of one receptor upon agonist binding to the other protomer. Heteromerization generates a paradigm shift in signal transduction by GPCRs: from vertical (one ligand, one receptor, one effector) to horizontal (two interacting receptors)[9]. It can be suggested that receptor heteromerization is a singular way in which the cell modulates signaling and physiological responses through allosteric interactions between receptors. These interactions may depend on the receptor environment and, therefore, different distributions of receptor heterodimers can be obtained depending on the brain region considered, as observed for mGlu2-mGlu4 heterodimers [28].

Receptor heterodimerization may open new opportunities in drug therapy, particularly in drug combination therapy, by taking advantage of the synergistic effects between drugs that appear through allosteric interactions between the two protomers in the receptor heterodimer. Drug combination therapy is widely used for different diseases being chronic pain a typical example [13]. Drug combination therapy includes the administration of two or more drugs, say two for simplicity, A and B, in which [A] + [B] added concentrations are more beneficial than either 2[A] or 2[B]. This may be of particular relevance in the case of chronic pain and the use of opioids as analgesics [11]. Due to the severe side effects of opioids, it may be advisable to use a two-drug combination (A, B) in which the opioid, say A, is added at a low concentration. The non-opioid drug, say B, which is assumed to produce less severe effects, would ideally interact cooperatively with A, thus facilitating that the decrease in the concentration of A does not reduce the desired therapeutic effect.

The concept of receptor heterodimerization provides a mechanistic framework for quantifying the biological response of two simultaneously acting drugs. In a previous publication, a mathematical model for heterodimeric receptors at equilibrium was proposed and the functional and binding response quantified [40]. In a subsequent study, binding kinetics was considered in the context of receptor heteromerization and under equilibrium conditions by converting dissociation equilibrium constants (K_n) into association (k_n) and dissociation (k_{-n}) rate constants, where $K_n = k_{-n}/k_n$ [7].

The main objective of the present study is to extend our previous studies [40,7] by adding the time variable to the heterodimer receptor model to quantitatively analyze the dynamic behavior of the different receptor species under non-equilibrium conditions. Our study also complements previous work modeling the binding of two ligands to a homodimeric receptor [37]. It is worth noting that since the chosen biological system is a heterodimeric receptor, the present study is appropriate for the quantification of the binding and functionality of two different drugs targeting two different receptors and then fits the purpose of drug combination therapy. This therapeutic approach requires the establishment of a solid conceptual framework so that proposed drug combinations are supported by rigorous mechanistic models and are not based solely on empirical data. In this sense, the formalism developed here could be of interest for experimenters to test hypotheses involving receptor-receptor interactions and also in pharmacokinetic/pharmacodynamic (PK/PD) studies to incorporate the increasing complexity currently appearing in molecular pharmacology.

2. Methods

The goal of this section is to present a dynamical system formed by ordinary differential equations (ODEs) that describes the behavior of binding kinetics of a heterodimeric receptor over time, and to explain how we deal with the solutions in two paradigmatic cases.

The rates of the forward and backward processes of each of the reversible ligand-receptor association/dissociation reactions included in Fig. 1 are obtained according to the Law of Mass Action. This law states that the rate v_n of any chemical reaction is equal to the product of the concentrations of the reactants times the corresponding microscopic rate constants k_n:

$$\begin{aligned} v_1 &= k_1[A]x, & v_{-1} &= k_{-1}y, \\ v_2 &= k_2[B]x, & v_{-2} &= k_{-2}z, \\ v_3 &= k_3[B]y, & v_{-3} &= k_{-3}w, \\ v_4 &= k_4[A]z, & v_{-4} &= k_{-4}w, \end{aligned} \tag{1}$$

where x = $[R_1R_2]$, y = $[AR_1R_2]$, z = $[R_1R_2B]$, w = $[AR_1R_2B]$, and [A] and [B] are the concentrations of the free ligands, respectively. The concentrations of the chemical species are expressed in molarity (M) and the forward and reverse rate constants in $M^{-1}\,s^{-1}$ and s^{-1}, respectively.

Then, according to Fig. 1, the global dynamics of the heterodimer model is represented by the following system of ODEs:

$$\begin{cases} x' = v_{-1} + v_{-2} - v_1 - v_2 = k_{-1}y + k_{-2}z - k_1[A]x - k_2[B]x, \\ y' = v_{-3} + v_1 - v_3 - v_{-1} = k_{-3}w + k_1[A]x - k_3[B]y - k_{-1}y, \\ z' = v_{-4} + v_2 - v_4 - v_{-2} = k_2[B]x + k_{-4}w - k_{-2}z - k_4[A]z, \\ w' = v_4 + v_3 - v_{-4} - v_{-3} = k_4[A]z + k_3[B]y - k_{-4}w - k_{-3}w, \end{cases} \tag{2}$$

where $x' = \frac{dx}{dt} = \frac{d[R_1R_2]}{dt}$, $y' = \frac{dy}{dt} = \frac{d[AR_1R_2]}{dt}$, $z' = \frac{dz}{dt} = \frac{d[R_1R_2B]}{dt}$ and $w' = \frac{dw}{dt} = \frac{d[AR_1R_2B]}{dt}$.

There are three constraints on this system. The first one is the conservation of the total receptor concentration, $[R_{tot}] = x + y + z + w$, which provides the dependence of any of the four variables on the other three. Without loss of generality, we choose to eliminate the variable w by substituting

$$w = [R_{tot}] - x - y - z. \tag{3}$$

Therefore, the four-dimensional ODE system (2) is reduced to the tridimensional ODE system

$$\begin{cases} x' = k_{-1}y + k_{-2}z - k_1[A]x - k_2[B]x, \\ y' = k_{-3}([R_{tot}] - x - y - z) + k_1[A]x - k_3[B]y - k_{-1}y, \\ z' = k_2[B]x + k_{-4}([R_{tot}] - x - y - z) - k_{-2}z - k_4[A]z. \end{cases} \tag{4}$$

The other two constraints are the conservation of the total concentrations of ligands A and B:

$$[A_{tot}] = [A] + [AR_1R_2] + [AR_1R_2B] = [A] + y + w,$$

$$[B_{tot}] = [B] + [R_1R_2B] + [AR_1R_2B] = [B] + z + w,$$

and so

$$[A] = [A_{tot}] - y - w, \tag{5}$$

$$[B] = [B_{tot}] - z - w. \tag{6}$$

By substituting the expression for w from equation (3) into equations (5) and (6) we get:

$$[A] = [A_{tot}] - [R_{tot}] + x + z, \tag{7}$$

$$[B] = [B_{tot}] - [R_{tot}] + x + y. \tag{8}$$

When relationships (7) and (8) are included in system (4), a general model for the heterodimer dynamics is obtained, in which the dependence on the total concentrations of both ligands and receptors will obviously play an important role. Since we want to explore the combined effect of the two ligands, we focus on specific cases of the general model. More precisely, we consider two cases:

- Case 1: both ligands are in excess with respect to the total receptor concentration. This case corresponds to a regular administration of drugs.
- Case 2: only one ligand is in excess with respect to the total receptor concentration. In this case, the dose of one of the drugs is reduced due to therapeutic reasons. This situation can be the case of an opioid drug because of its unwanted side effects such as respiratory depression, constipation or addiction.

For Case 1, the following approximations hold:

$$[A_{tot}] \gg [R_{tot}] \Rightarrow [A] \approx [A_{tot}] \tag{9}$$

$$[B_{tot}] \gg [R_{tot}] \Rightarrow [B] \approx [B_{tot}] \tag{10}$$

Consequently, model (4) becomes

$$\begin{cases} x' = k_{-1}y + k_{-2}z - k_1[A_{tot}]x - k_2[B_{tot}]x, \\ y' = k_{-3}([R_{tot}] - x - y - z) + k_1[A_{tot}]x - k_3[B_{tot}]y - k_{-1}y, \\ z' = k_2[B_{tot}]x + k_{-4}([R_{tot}] - x - y - z) - k_{-2}z - k_4[A_{tot}]z. \end{cases} \tag{11}$$

Observe that system (11) is a linear system of ODEs. Thus, we can take advantage of the extensive knowledge provided by the theory of linear ODEs.

For Case 2, we will assume that ligand B is in excess with respect to the total receptor concentration, while concentration of ligand A is several orders of magnitude lower. Thus, by substituting equations (7) and (10) for the concentrations of ligands A and B, respectively, in (4), we obtain the following system:

$$\begin{cases} x' = k_{-1}y + k_{-2}z - k_1([A_{tot}] - [R_{tot}] + x + z)x - k_2[B_{tot}]x, \\ y' = k_{-3}([R_{tot}] - x - y - z) + k_1([A_{tot}] - [R_{tot}] + x + z)x - k_3[B_{tot}]y - k_{-1}y, \\ z' = k_2[B_{tot}]x + k_{-4}([R_{tot}] - x - y - z) - (k_{-2} + k_4([A_{tot}] - [R_{tot}] + x + z))z. \end{cases} \tag{12}$$

In this case, the system is non-linear (in fact, quadratic) and we will have to resort to qualitative and numerical methods.

3. Results

As stated in Methods, two conditions were considered, namely, both ligands are in excess (Case 1) and only one is in excess (Case 2) with respect to the total receptor concentration.

3.1. Case 1: Both ligands are in excess with respect to the total receptor concentration

As mentioned above, the model for this case, system (11), is linear: it can be expressed as X' = MX + b, where $X = (x,y,z)^T$, M is a 3x3 matrix and b a 3x1 vector. The theory of linear systems of differential equations is well-established (see, for instance, [35]) and it is possible to obtain explicit expressions of the solutions of the system, that is, exact algebraic descriptions of the time evolution of the concentrations of all the species involved in the model. Anyway, given that the number of parameters (eleven) is large enough, the expressions are very long and showing them does not provide a better understanding of the results; we refer to Section 3.1 of [27] for an explanation of how to obtain these long expressions. Alternatively, we will focus on providing information on relevant qualitative aspects and numerical simulations.

System (11) has a unique equilibrium point (since the determinant of M is not null; see Appendix A), which has all coordinates positive and is stable for any combination of the parameter values (k_i), provided that they are positive. Proving that all coordinates are positive is immediate

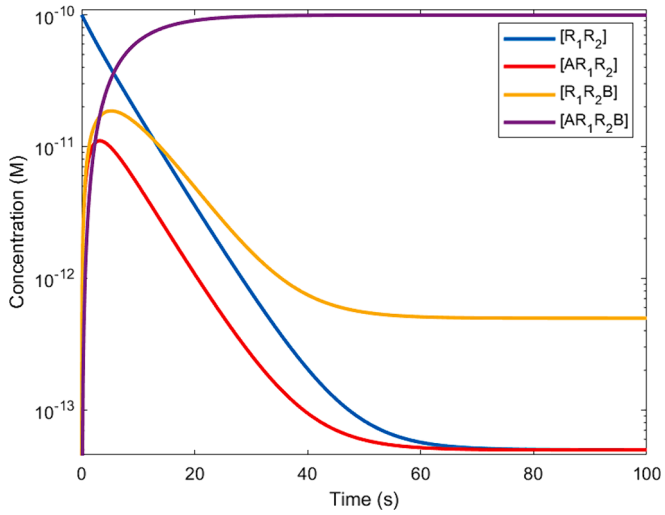

Fig. 2. Evolution of the four heterodimeric receptor species over time when both ligands A and B are in excess with respect to the total receptor concentration. Parameter values were taken from [7]: $[R_{tot}] = 10^{-10}$ M, $[A_{tot}] = [B_{tot}] = 10^{-8}$ M, $k_1 = k_2 = 10^7$ $M^{-1}s^{-1}$, $k_{-1} = 10^{-1}$ s^{-1}, $k_{-2} = 10^{-2}$ s^{-1}, $k_3 = 4 \cdot 10^7$ $M^{-1}s^{-1}$, $k_{-3} = 2 \cdot 10^{-4}$ s^{-1}, $k_4 = 2 \cdot 10^7$ $M^{-1}s^{-1}$, $k_{-4} = 10^{-3}$ s^{-1}. Initial condition: all heterodimers are empty, $(x_0, y_0, z_0) = ([R_{tot}], 0, 0)$.

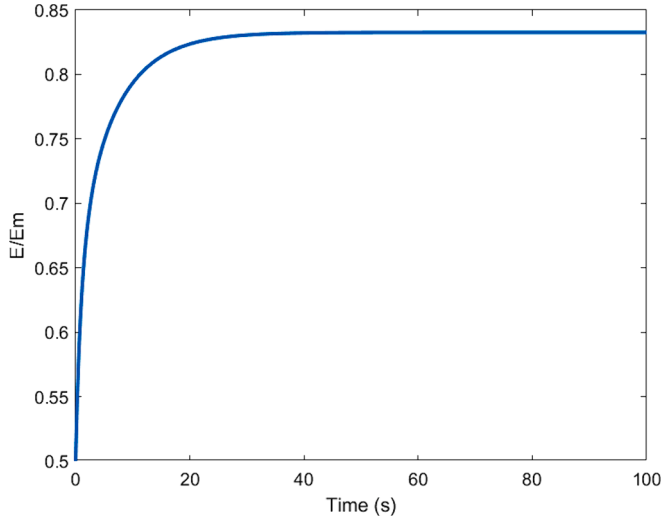

Fig. 3. Evolution of the fractional response over time when both ligands A and B are in excess with respect to the total receptor concentration. Parameter values for binding kinetics are the same as in Fig. 2, and the rest are the following, taken from [7]: $K_E = 10^{-10}$ M, $\varepsilon = 1$, $\varepsilon_A = 10$, $\varepsilon_B = 10^{-1}$, $\delta = 5$ and $\varepsilon_{AB} = \delta\varepsilon_A\varepsilon_B = 5$. The effect increases monotonically from basal response ($E/E_m = 0.5$) until it reaches equilibrium asymptotically just as the concentrations of the different receptor species. Note that the basal response is $\frac{E}{E_m} = \frac{\frac{\varepsilon[R_{tot}]}{K_E}}{\frac{\varepsilon[R_{tot}]}{K_E}+1} = \frac{1}{2}$ [40].

once the general expression of the equilibrium point is obtained. Instead, ensuring stability for any choice of the parameters is not trivial as it requires the application of the Routh-Hurwitz theorem (see Appendix A for details). The uniqueness and stability of the equilibrium point guarantees that, upon setting fixed values for the system's parameters, regardless the choice of the initial concentrations, the same equilibrium will invariably be attained.

Fig. 2 depicts the evolution of the concentrations of the four receptor species over time for a particular set of parameter values. These values have been chosen as a reference example to visualize how the pharmacological model responds to particular established conditions. Initially, at $t = 0$, the only receptor species is the free receptor and the ligands A and B are both unbound with their concentrations being equal to the externally supplied concentrations. As time increases, the concentration of the free receptor (blue curve) decreases monotonically whereas the singly bound receptor species (red and yellow curves) increase till reaching a maximum and then decrease; the doubly bound receptor species (violet curve) increases monotonically. For $t \to \infty$ or, in practical terms, for sufficiently large times, the four receptor species reach the equilibrium values, as expected. These equilibrium values can be also obtained by setting all the right-hand side components of system (11) equal to zero and solving for x, y and z. Concentrations values at equilibrium are $x_{eq} = 4.97 \cdot 10^{-14}$ M, $y_{eq} = 4.97 \cdot 10^{-14}$ M, $z_{eq} = 4.97 \cdot 10^{-13}$ M and $w_{eq} = 9.94 \cdot 10^{-11}$ M for the set of parameter values chosen in Fig. 2. By the conservation law (3), the sum of the concentrations of the four receptor species equals the initial free receptor concentration. Because ligands A and B are in excess with respect to the receptor concentration, they are not significantly consumed over time and, at equilibrium, their concentrations are practically the same as at time zero.

Analysis of the time-dependent concentration curves in Fig. 2 in terms of the values of the chosen parameters allows the binding cooperativity between ligands A and B to be examined. Indeed, in the same way as the ratio between rate constants produces equilibrium constants, the ratio between cooperativity rate constant parameters produces binding cooperativity parameters. In the present case, notice that $\alpha_+ = 2$, $\alpha_- = 10^{-2}$, $\beta_+ = 4$, $\beta_- = 2 \cdot 10^{-2}$ and, then, $\alpha_+/\alpha_- = \alpha = \beta_+/\beta_- = \beta = 200$, which implies a positive binding cooperativity between A and B across the heterodimer interface. Now, considering that the equilibrium dissociation constants corresponding to Fig. 2 are $K_1 = [A]_{eq}[R_1R_2]_{eq}/[AR_1R_2]_{eq} = 10^{-8}$ M, $K_2 = [B]_{eq}[R_1R_2]_{eq}/[R_1R_2B]_{eq} = 10^{-9}$ M, $K_3 = K_2/\beta = [B]_{eq}[AR_1R_2]_{eq}/[AR_1R_2B]_{eq} = 5 \cdot 10^{-12}$ M and $K_4 = K_1/\alpha = [A]_{eq}[R_1R_2B]_{eq}/[AR_1R_2B]_{eq} = 5 \cdot 10^{-11}$ M, where the concentrations of the different species are taken at equilibrium, the equality $\alpha = \beta = 200$ means that the affinity of ligand A or B for its respective protomer in the heterodimer is 200 times higher when the other protomer is occupied. It is worth mentioning that this result can be obtained through an infinite number of combinations of rate constants satisfying $\alpha_+/\alpha_- = \beta_+/\beta_- = 200$. In the example taken for Fig. 2, what differentiates ligands A and B is the dissociation rate constant for their respective protomers (k_{-1} and k_{-2}), which is 10 times lower for ligand B. This value allows for differentiation between the time-dependent curves for $[AR_1R_2]$ and $[R_1R_2B]$.

Binding kinetics [16,18,21,36] can be connected to the pharmacological response, E, through a transduction function depending on the generated stimulus, S [40]:

$$\frac{E}{E_m} = \frac{S}{K_E + S}, \tag{13}$$

where E_m is the maximum possible effect of the system and the ratio E/E_m is the *fractional response*. The parameter K_E represents the stimulus that produces half E_m. The stimulus S is the sum of the stimuli generated by all heterodimeric receptor species, which are defined as the product of their concentrations times their intrinsic efficacies ε_i:

$$S = \epsilon[R_1R_2] + \epsilon_A[AR_1R_2] + \epsilon_B[R_1R_2B] + \epsilon_{AB}[AR_1R_2B]. \tag{14}$$

These equations allow modeling the time-dependent effect of a heterodimer receptor from the initial time (unbound receptors) until equilibrium is reached. Fig. 3 depicts the fractional response of a receptor heterodimer by using the binding kinetics parameters included in Fig. 2 and the functional parameters $K_E = 10^{-10}$ M, $\varepsilon = 1$, $\varepsilon_A = 10$ and $\varepsilon_B = 10^{-1}$. The functional parameter values have been chosen so that A is an agonist ($\varepsilon_A > \varepsilon$), B is an inverse agonist ($\varepsilon_B < \varepsilon$) and there is a positive functional cooperativity between the two ligands $\varepsilon_{AB} = \delta\varepsilon_A\varepsilon_B > \varepsilon_A\varepsilon_B$, or $\delta > 1$ (in this case, $\delta = 5$). As for the binding kinetics part, these values have been chosen as a reference example to visualize how the

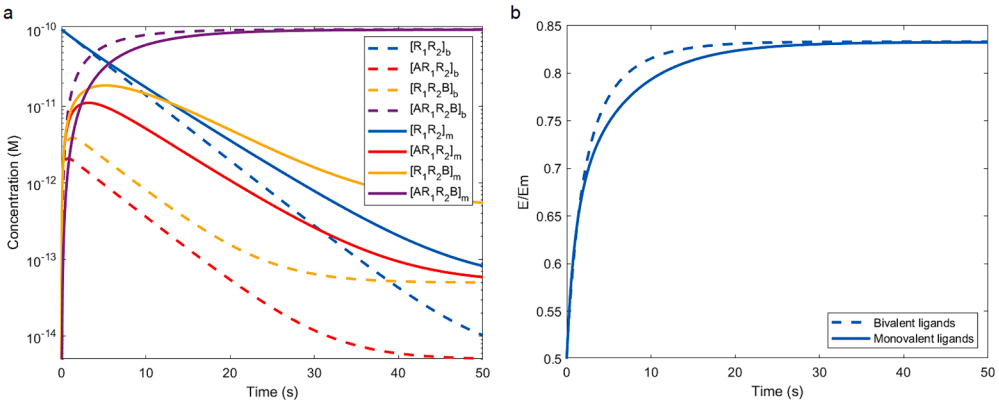

Fig. 4. a) Evolution over time of the four heterodimeric species when A and B are the pharmacophores of a bivalent ligand AB in comparison with monovalent A, B ligands (Fig. 2). The initial condition and the parameter values are the same as in Fig. 2, except k_3 and k_4, which are multiplied by 10 in the bivalent case, taking now the values of $4 \cdot 10^8\ M^{-1}\ s^{-1}$ and $2 \cdot 10^8\ M^{-1}\ s^{-1}$, respectively. Solid lines (subscript m in concentration legends) correspond to monovalent ligands whereas dashed lines (subscript b in concentration legends) correspond to bivalent ligands. b) Comparison of fractional response between bivalent and monovalent ligands (see Fig. 3). Functional parameters are the same as in Fig. 3. It is worth noting that, after the change in k_3 and k_4 by increasing α_+ and β_+ ten times, the condition $(k_{-1}\ k_4)/(k_1\ k_{-4}) = (k_{-2}\ k_3)/(k_2\ k_{-3})$, or $\alpha_+/\alpha_- = \beta_+/\beta_-$, is still valid.

pharmacological model responds to particular established conditions. The values used for the efficacy parameters are compatible with a bivalent ligand that included two scaffolds: a MOP agonist (here, ligand A) and a CB1 inverse agonist (here, ligand B), which proved to have antinociceptive properties when the scaffolds were linked by a spacer of a particular length [24]. Selective effects elicited by bivalent ligands are indicative of heterodimeric receptors. Thus, the pharmacological profiles and parameter values used in the present study seem plausible in the context of a heterodimeric receptor with chronic pain as the proposed therapeutic target.

Note that the fractional effect increases monotonically from basal response at time zero and reaches a plateau of 0.83, which means that the observed response is equivalent to that of a partial agonist in a monomeric receptor.

3.1.1. *Bivalent ligands*

The transient or stable presence of receptor heterodimers in the cell membrane immediately suggests the possibility of synthesizing bivalent ligands. Ideally, these molecules would include two pharmacophores specially designed for the corresponding protomers in the heterodimer and a linker with sufficient length to simultaneously attach the two pharmacophores to both binding sites [20,30,32]. Because pharmacophores A (to bind R_1) and B (to bind R_2) are constantly linked forming the bivalent AB molecule, we cannot consider the case where A and B have different total concentrations (Case 2, see Section 3.2). Because of this, only Case 1 will be included in this study.

An ideal bivalent AB molecule differs in binding terms from the combination of two monovalent molecules (A, B) in that once one of the two pharmacophores (say A) has bound to its corresponding protomer (R_1), the second pharmacophore (B) has a higher probability of binding with respect to the monovalent case. The reason for this fact is the greater proximity of the free pharmacophore to the second protomer in the heterodimer (once the first protomer is occupied), which is caused by a linker with the right length. This results in an increase of global affinity with respect to the monovalent case, that is, in an increase of the α_+ and β_+ cooperativity rate constant parameters (defined in Fig. 1b). Therefore, the rate constants $k_3 = \beta_+\ k_2$ and $k_4 = \alpha_+\ k_1$ in system (11) will have the same relative increment. Thus, if the monovalent case has positive cooperativity, it is clear that cooperativity in the bivalent case remains positive; if monovalent A, B ligands display negative cooperativity then the increment of cooperativity provided by the bivalent ligand might or might not be sufficient to reverse the sign of the cooperativity.

It is also worth noting that the possibility that bivalent ligands can increase the relative population of heterodimers is not contemplated herein because the model (Fig. 1) assumes that heterodimers are already preformed and so R_1 and R_2 monomers are not present in the system. This assumption precludes the complexity of monomeric and heteromeric receptors coexisting in the system.

According to the previous considerations, in order to simulate the bivalent case (see Fig. 4), we consider k_3 and k_4 to be ten times greater for the bivalent ligand AB than for the monovalent ligands A, B (studied in Fig. 2). Notice that these changes do not affect the condition $(k_{-1}\ k_4)/(k_1\ k_{-4}) = (k_{-2}\ k_3)/(k_2\ k_{-3})$ that binds the values of the rate constants at equilibrium [7]. Dashed curves in Fig. 4a, which includes the curves previously depicted in Fig. 2 (solid lines) for easier comparison, show faster dynamics in the bivalent case since all the species tend to reach their equilibrium values more rapidly. Also, curve peaks of $[AR_1R_2]$ and $[R_1R_2B]$ are lower when A and B are part of a bivalent ligand because AR_1R_2B is formed earlier. In addition, equilibrium concentrations of R_1R_2, AR_1R_2 and R_1R_2B decrease by one order of magnitude in the bivalent case with respect to the monovalent one. On the other hand, Fig. 4b shows that the fractional pharmacological response increases monotonically and reaches practically the same value independently of whether A and B are monovalent ligands or part of a bivalent compound. However, the equilibrium value is reached faster in the latter case.

3.2. *Case 2: Only one ligand (B) is in excess with respect to the total receptor concentration*

Case 2 results from the need of decreasing the concentration of one of the ligands (say ligand A) in the proposed two-drug combination therapy. This decision can be due to the fact that ligand A exerts unwanted side effects when it is used as a single drug at therapeutic concentrations. To exemplify this, we are considering that ligand A is an opioid and that chronic pain is the therapeutic target. In our heterodimer model the compensation in ligand efficacy because of low A concentrations is obtained through the allosteric effects elicited by ligand B.

For Case 2, as mentioned in the Methods section, the mathematical model, system (12), is not linear but quadratic. For the linear case, we have shown that the existence of a single equilibrium point is guaranteed by definition and, using the Routh-Hurwitz criterion, we have been able to determine its stability for any combination of microscopic rate constants. Unfortunately, for quadratic systems uniqueness of equilibria is not guaranteed and, moreover, the application of criteria that ensure their stability is much more laborious, mostly when there are so many parameters involved. In fact, their study is part of the study of the properties of reaction networks, which has been developed in the last

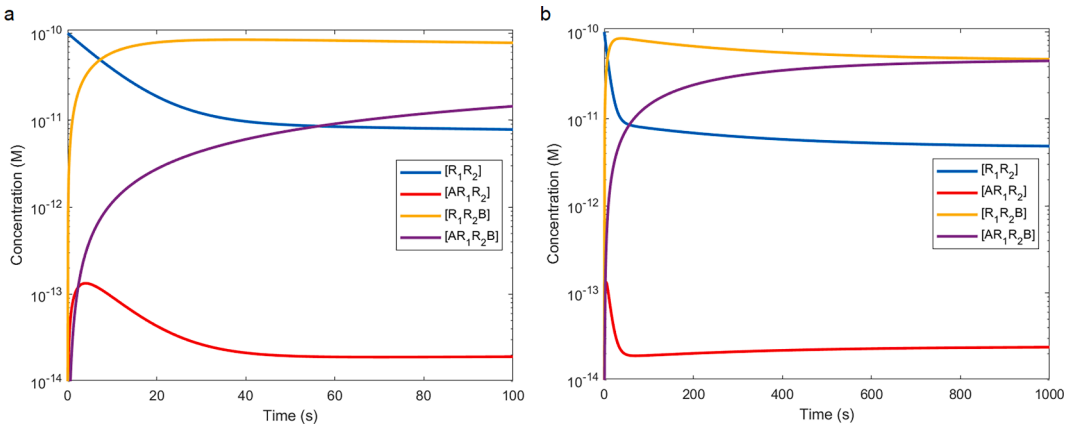

Fig. 5. Evolution of the concentrations of the four heterodimeric species over time when only ligand B is in excess with respect to the total receptor concentration. Parameter values and the initial condition are the same as in Fig. 2, except $[A_{tot}]$ which takes here the value of 10^{-10} M. a) First 100 s. b) First 1000 s. Subfigure a) is a zoom of the first part of Subfigure b).

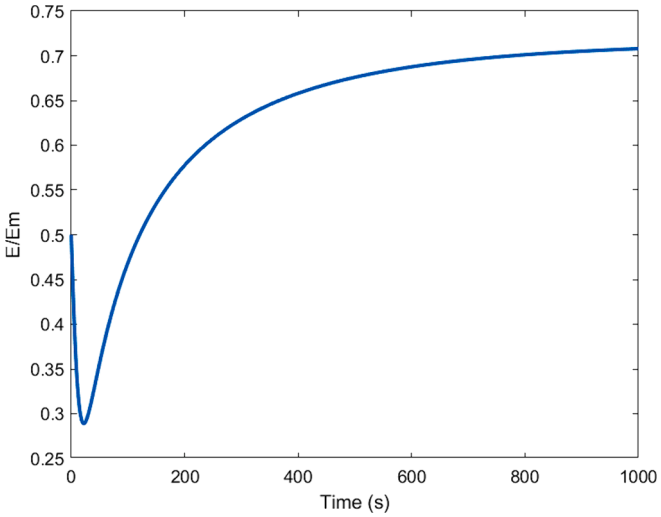

Fig. 6. Evolution of fractional biological response E/E_m over time when only ligand B is in excess with respect to the total receptor concentration. Parameter values for binding kinetics are the same as in Fig. 5, and functional parameters are the same as in Fig. 3.

half-century (see, for example, [8]).

In this paper, we use a more parsimonious approach. Since we want to illustrate the combined effect of two ligands under biologically plausible conditions for the heterodimer, we choose a particular realistic set of rate constants (already shown in Fig. 2) to illustrate the study. We then compute the equilibria of system (12) for this particular choice of parameters. It can be shown (see Appendix B) that there are three equilibrium points. Notice that only one of them belongs to the first octant (i.e., $x > 0$, $y > 0$ and $z > 0$) and, moreover, it is stable (proved in Appendix B). The coordinates of this point are $x_{eq} = 4.69 \cdot 10^{-12}$ M, $y_{eq} = 2.42 \cdot 10^{-14}$ M, $z_{eq} = 4.69 \cdot 10^{-11}$ M and $w_{eq} = 4.84 \cdot 10^{-11}$ M.

In addition to this numerical identification and classification, we develop a theoretical argument that ensures that this positive equilibrium will persist and none of the other two can become positive by changing the parameter values. Note that different drugs, different properties of interaction between species, different initial concentrations or even different experimental conditions imply different choices of parameters and, therefore, it is desirable to be able to guarantee that the results are applicable in a sufficiently wide region of the parameter space. In other words, a result that was only true for a specific choice of parameters and specific initial conditions would not be useful since any small variation in the experiment or any measurement error would invalidate the conclusions. For this purpose, we provide an analytical proof that there exists a positively invariant region in the first octant for all combinations of positive constant rate parameters (see Appendix C). This implies that (i) for any initial condition (initial values of the

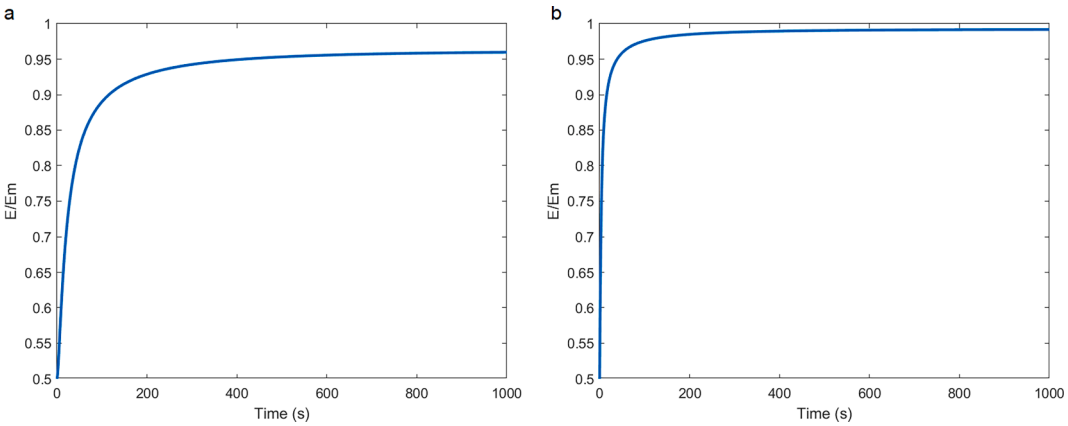

Fig. 7. Evolution of the fractional biological response over time when only ligand B is in excess with respect to the total receptor concentration. Parameter values for binding kinetics are the same as in Fig. 5, and functional parameters are the same as those in Fig. 3, except ε_B. a) $\varepsilon_B = \varepsilon = 1$ (B is a neutral antagonist). b) $\varepsilon_B = 5$ (B is an agonist).

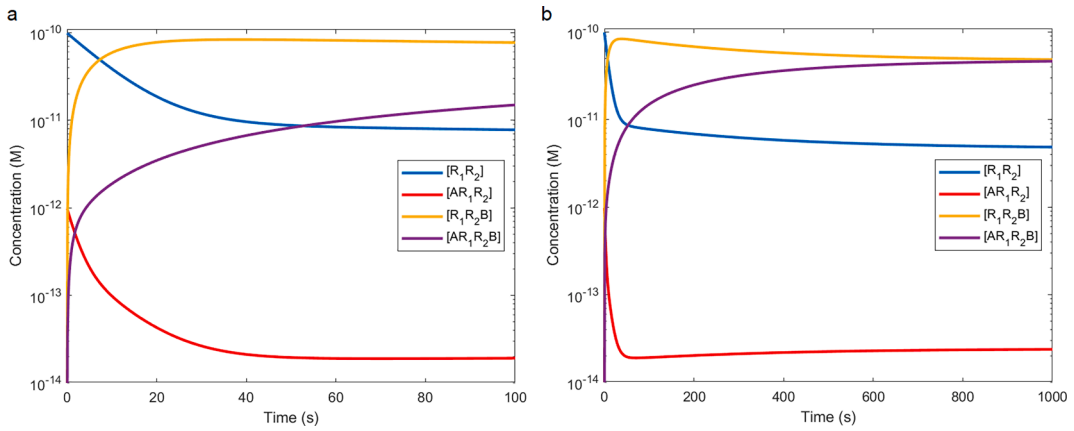

Fig. 8. Evolution of the four heterodimeric species over time under the condition that A is an endogenous ligand and then is already present in the system at t = 0. The new initial condition is $(x_0, y_0) = (9.902 \cdot 10^{-11}$ M, $9.805 \cdot 10^{-13}$ M). Parameter values are the same as in Fig. 5. a) First 100 s. b) First 1000 s. Subfigure a) is a zoom of the first part of Subfigure b).

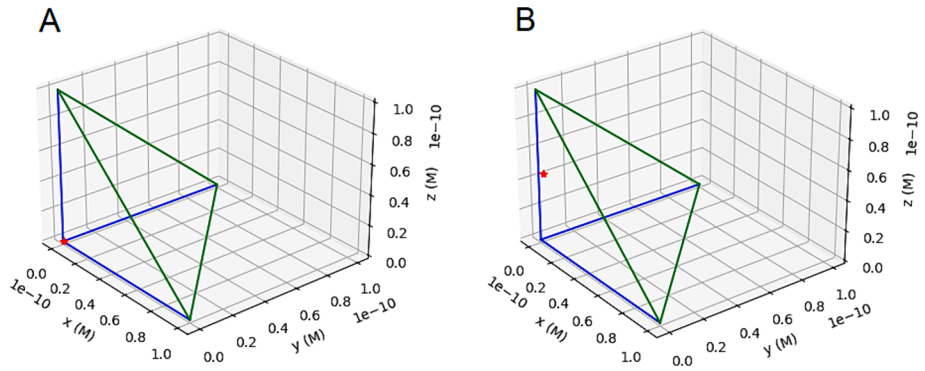

Fig. C1. Tetrahedral positively closed invariant region for the two pharmacological conditions described above: (a) both ligands are in excess (Case 1) and (b) only one of them is in excess (Case 2). Blue lines represent the three coordinated axes and the green triangle represents the intersection of the plane $ax + by + cz = d$ with the three coordinate planes. Red stars represent equilibrium points (attractors, in both cases).

concentrations) within this region, the dynamics remains inside it, and (ii) none of the other equilibria can enter the first octant continuously in parameter space. Consequence (ii) prevents from having multistationarity. Once the existence of multiple stable points is excluded, consequence (i) tells us that, unless other more complicated behaviors (for instance, oscillations) occur, the positive equilibrium detected in the particular example will be an attractor for all trajectories, that is, its coordinates will be the limit value of the corresponding concentrations; of course, the coordinates of the equilibrium point will depend on the values of the parameters k_i. Summarizing, with this construct we provide strong evidence that the situation described in this particular example is representative of the situation in the whole parameter space for Case 2. In this way, we ensure the robustness and applicability of our conclusions.

Fig. 5 depicts the evolution over time of the concentrations of the four receptor species. The same parameter values as those used in Fig. 2 are considered except for the total concentration of ligand A, which is now the same as that of the total receptor concentration (that is, 10^{-10} M), thus being not in excess. Although Case 2 is more complex than Case 1 (both ligands in excess with respect to the total receptor concentration), at the end the situation of having a single biologically plausible equilibrium makes the general picture of the two cases qualitatively similar. However, there are significant differences in both the time scale and the variable y ($[AR_1R_2]$ concentration) as it can be noticed if we compare Fig. 5 to Fig. 2. It is worth mentioning that since $[AR_1R_2]$ (red curve) is very low compared to the other chemical species, the y-axis in Fig. 5 is in logarithmic scale in order to be able to observe the curve properly.

Following the same thread as in the previous section, binding kinetics can be connected to pharmacological response through the transduction function of the generated stimulus S (see equations (13) and (14)). Fig. 6 depicts the fractional response for this situation assuming the same functional parameters as those used in the previous example.

It can be seen that at t = 0 the same basal response as in the previous case is found ($E/E_m = 0.5$). Interestingly, a decrease of the response is now observed. This decrease can be explained by the formation of $[R_1R_2B]$, with B acting as an inverse agonist. The very low concentration of $[AR_1R_2]$ makes irrelevant its contribution to function. The fractional response decreases until AR_1R_2B, which behaves as an agonist, counteracts the effect of R_1R_2B. Finally, as time increases, an equilibrium value reflecting partial agonism is obtained.

Of note, the minimum described in Fig. 6 disappears if we consider that ligand B is a neutral antagonist (Fig. 7a) or an agonist (Fig. 7b). In both cases, fractional response increases monotonically until a plateau is reached. The difference between these two situations lies in the value of the plateau and the time required to reach it: if B is an agonist ($\varepsilon_B > \varepsilon$), the plateau is reached faster and takes almost the value of the maximum fractional response (1); however, if B is a neutral antagonist ($\varepsilon_B = \varepsilon$), then the plateau is reached more slowly and gets a value a bit lower (around 0.96).

3.2.1. *The ligand that is not in excess is an endogenous ligand*

The examples developed above have been proposed under the

assumption that A and B are exogenous ligands and, because of that, the receptor is empty at t = 0. However, it can be considered that one of the ligands, for instance, the one at low concentration (ligand A), is an endogenous ligand and, for this reason, $[AR_1R_2]$ is not zero at t = 0. Some examples of this situation could be the endocannabinoid [26] or the endogenous opioid [2] systems. We will assume, as above, that B is added externally.

We can solve the system assuming that at t = 0 there is an equilibrium between the endogenous ligand A and the receptor heterodimer R_1R_2, which can be represented as:

$$A + R_1R_2 \underset{k_{-1}}{\overset{k_1}{\rightleftarrows}} AR_1R_2 \tag{15}$$

The time dynamics of this binary binding process is described by

$$\frac{dx}{dt} = k_{-1}([R_{tot}] - x) - k_1 x(x + [A_{tot}] - [R_{tot}]). \tag{16}$$

Since this process is supposed to be at equilibrium, the initial condition (x_0, y_0, 0) for the process in which B is added externally is obtained by solving for x the right-hand side of equation (16) and using that the conservation law $x_0 + y_0 = [R_{tot}]$:

$$x_0 = \frac{k_{-1} + k_1[A_{tot}] - k_1[R_{tot}] - \sqrt{\left(k_{-1} + k_1[A_{tot}] - k_1[R_{tot}]\right)^2 + 4k_1k_{-1}[R_{tot}]}}{-2k_1}, \tag{17}$$

$$y_0 = [R_{tot}] - x_0. \tag{18}$$

As we can observe in Fig. 8, and compared to Fig. 5, differences are barely perceptible, apart from the new y_0. This is due to the low concentration of ligand A with respect to the total receptor concentration (not many receptors will be previously half-occupied by A), and also because the system dynamics is the same: the system tends to reach its unique equilibrium point as time goes on.

4. Discussion

Drug combination therapy is a logical approach to address the complexity of many diseases. This complexity may result from the interactions between cellular components of an organism that form extensive networks. These networks regulate subcellular functions that are characteristic of both health and disease. Networks can be at the cellular, tissue and organ levels. Drugs typically act at the molecular level by changing the activity of the molecular components, and this change translates to higher levels of organization correcting organismal malfunctions in disease states, and giving rise to the field of systems pharmacology [22]. Cooperativity effects between two drugs through physical interactions between the two protomers that form a receptor heterodimer can be considered the simplest case of systems pharmacology.

There is increasing evidence for the existence of receptor oligomerization and, in particular, of receptor heterodimerization (see [9] and references therein), although this proposal has given rise to intense debates because class A GPCRs can be functional as monomers [4,23]. Thus, receptor heteromerization can be considered as a particular case of allosterism through protein–protein interactions that are transient in Class A GPCRs and stable in Class C GPCRs [25,28,29]. Nevertheless, caution should be taken when hypothesizing receptor heteromerization from functional studies because, as stated in [31], crosstalk can result not only from receptor oligomerization, but also from colocalized receptor sharing signaling pathways, or from synergistic regulation of signaling crossroads, independently of oligomerization.

Being aware of the complexity of GPCR signaling and the many structural and functional components involved in cellular networks, the time-dependent model for a ligand-receptor heterodimeric receptor included in this article may represent a significant contribution to the field. The model is of general applicability to any combination of receptors addressing any disease but to exemplify we have focused on chronic pain and, in particular, on heterodimers in which one of the protomers is MOP. Some studies can be found in the literature exploring MOP heteromerization by using bivalent ligands constituted by a MOP selective agonist, a pharmacophore selective for the other protomer and a spacer connecting both. These studies included amongst others the MOP-DOP [6], the MOP-CB1 [24] and the MOP-mGlu5 [1] heterodimers. Administration of bivalent ligands targeting MOP-DOP, MOP-CB1, or MOP-mGlu5 heteromers produced antinociception that was greater than that observed with morphine but without side effects such as tolerance, dependence, or respiratory depression [15]. Interestingly, in these three cases the pharmacophore selective for the partner protomer of MOP in the heterodimer was an inverse agonist. It is expected that these combinations of ligands with an agonist for R_1 and an inverse agonist for R_2 would lead to an asymmetric R_1*R_2 active state (R_1 active and R_2 inactive) with R_1 being MOP and R_2 the partner protomer. It can be proposed that the inverse agonist bound-R_2 inactive protomer stabilize the agonist-bound R_1 active protomer leading to a structural heterodimer with distinct functional properties. Thus, it can be considered that R_2, and with greater potency the inverse agonist-bound R_2, acts as an allosteric modulator of the agonist-bound R_1. Interestingly, and in line with this proposal, a combination of an mGlu2 (a Class C GPCR) agonist with a 5HT2AR (a Class A GPCR) inverse agonist was suggested as a potential drug combination therapy for schizophrenia patients for whom a suboptimal signaling balance between Gi and Gq proteins exists [10]. Of note, yet in an homodimeric context, an insightful modeling analysis on the asymmetric/symmetric activation of dimeric receptors can be found in [33]. See also [40] for the modeling of the binding and function of a heterodimeric receptor at equilibrium and [14] for an analysis of the function of receptor oligomers by operational models of agonism.

In this article we propose a model for the time-dependent ligand-receptor binding kinetics and functionality of a preformed heterodimeric receptor R_1R_2 that includes two ligands, A and B, that bind R_1 and R_2, respectively. The system was analyzed under two conditions: A and B are in excess with respect to the total receptor concentration (Case 1) and only one ligand, say B, is in excess (Case 2). Because of the data on bivalent ligands described above, we decided to perform our simulations initially assuming that ligand A is an agonist that binds to the first protomer R_1 (MOP) and B is an inverse agonist that binds to the second protomer R_2. In a second set of simulations, and to illustrate some of the varying synergistic effects that B may exert on the observed response, B was given intrinsic efficacies of a neutral antagonist or an agonist without changing the rest of the parameters. As a particular case of Case 2, the possibility that the ligand that is not in excess is an endogenous ligand was also considered (section 3.2.1.). Finally, the situation in which A and B are part of a bivalent ligand (section 3.1.1.) was examined in comparison with Case 1 in which A and B are monovalent ligands.

For Case 1, it can be seen that the doubly-occupied heterodimer, AR_1R_2B, tends to reach almost the 100 % of the total receptor concentration as time increases (Fig. 2), and this is achieved through the previous formation and disappearance of the singly-occupied receptors, AR_1R_2 and R_1R_2B, which both reach a concentration peak. The difference in shape of the two peaks is due to the difference in the microscopic dissociation rate constants k_{-1} and k_{-2} of the singly-bound receptors, considering that they bear the same values for the association rate constants k_1 and k_2. Because residence time is higher for lower values of the dissociation rate constant, and the microscopic dissociation rate constant of R_1R_2B (k_{-2}) is lower than that of AR_1R_2 (k_{-1}), the peak of R_1R_2B is higher and vanishes more slowly than that of AR_1R_2.

For Case 2, the difference in the initial concentrations of A (10^{-10} M) and B (10^{-8} M) affects the relative binding of both drugs to the heterodimer (Fig. 5). At the beginning, ligand B is the first to bind R_1R_2 and A

binds later. Because of the difference in ligand concentrations and being $k_1 = k_2$ and $k_{-2} < k_{-1}$, a big difference in the shape of the curves of the singly-bound receptors is observed, with a high peak for R_1R_2B at the beginning of this simulation. After that, $[R_1R_2B]$ decreases because A binds, causing a slow rising of $[AR_1R_2B]$. This slower time dynamics of the system for reaching the asymptotic value of $[AR_1R_2B]$ (around 1000 s) compared to the corresponding one in Fig. 2 (around 40 s) can be explained through the lower concentration of ligand A: since B is more abundant (by two orders of magnitude), encounters between A and receptors are not as frequent as with ligand B, so it takes longer for A to bind.

Comparing Figs. 5 and 6, it can be seen that the time value for the maximum in $[R_1R_2B]$ coincides with the minimum for the biological effect. This is because B is an inverse agonist (the intrinsic efficacy of R_1R_2B (ε_B) is lower than that of R_1R_2), leading to a decrease of the basal response when the predominant receptor species is R_1R_2B. When $[R_1R_2B]$ decreases and $[AR_1R_2B]$ forms, the effect recovers and keeps increasing until equilibrium is reached. The intrinsic efficacy of the doubly-occupied heterodimer AR_1R_2B is higher than that of R_1R_2, which means that the combination of ligands A and B behaves as an agonist entity and causes an effect higher than the basal. The overall effect elicited by the heterodimer due to the combination of the two ligands is similar to the effect of a partial agonist in a single receptor, because it is higher than that resulting from constitutive receptor activity, but it does not reach the maximum possible effect (E_m). This is because at equilibrium there is a mixture of R_1R_2B (inverse agonist) and AR_1R_2B (agonist); notice that $[AR_1R_2]$ is negligible.

Simulations under Case 2 have been performed under the premise that A is an opioid drug whose concentration is necessary to lower because of its unwanted side effects. This has been done by adding a second drug B that binds the partner protomer in a heterodimeric receptor that although is an inverse agonist for the single R_2 receptor behaves as an agonist when combined with A in the receptor heterodimer. Parameter values have been chosen to illustrate the many binding and functional responses that can be obtained. Experiments with controlled experimental design may help to obtain realistic and interpretable parameter values.

Case 2 was extended to consider also the situation in which A is not a compound externally added to the system but an already present endogenous ligand (section 3.2.1.). In this case, at $t = 0$ the total receptor concentration includes both the free R_1R_2 and the ligand-bound AR_1R_2 at equilibrium. Simulations were performed under this premise, which can be useful for therapeutic purposes. It can be agreed that taking advantage of all the chemical resources endogenously present in the system to avoid an excessive manipulation of living organisms seems a prudent pharmacotherapeutic strategy that, in principle, should be more devoid of side effects.

The possibility that A and B are not independent molecules but part of a bivalent ligand was also considered (section 3.1.1.) by increasing the cooperativity of binding (and so, the affinity) of the free pharmacophore when the other pharmacophore is already bound. This is due to the forced proximity of the free pharmacophore to its protomer in the heterodimer. The simulations performed showed faster dynamics for the bivalent case than for the monovalent one: the doubly-bound AR_1R_2B receptor species is formed more rapidly and the peak values of the singly-bound receptor species are lower. The binding effects associated to bivalent ligands are also reflected in the pharmacological response as simulations show (Fig. 8b).

Our model relates to the two-ligand and one-receptor model proposed in [37], where both ligands bind to the same receptor R (here, we consider two different receptors) but also allowing binding of a same ligand to two different receptor sites. Consequently, their model is a five-dimensional ODE system whose variables correspond to the species AR, BR, ARA, ARB and BRB. The two models complement each other. In particular, constraining our model to the case $R_1 = R_2$ and preventing the ligands A and B from competing for the same receptor, we obtain a subcase of White & Bridge's model. For this case, we have tested the coincidence of the solutions. However, the condition imposed in our study that A and B bind specifically to two different receptors, R_1 and R_2, seems more consistent with the application to drug combination therapy targeting two different receptors.

4.1. Conclusion

We have added the time variable to a previous heterodimeric receptor model at equilibrium [40]. The time-dependent model shows a single biologically plausible stable equilibrium point which lies in an invariant region for any combination of the parameter values, that is, any combination of microscopic rate constants. Hence, the results obtained here ensure a typical pharmacological scenario when exploring the optimal set of rate constants for a specific drug combination therapy [19]. The time dynamics of the biological response showed different behaviors depending on the intrinsic efficacies of the four heterodimeric species, and this can be used to explore the potential utility of drug combinations. This is particularly interesting when a dose reduction is desired for a drug causing unwanted side effects (such as an opioid drug) but avoiding the loss of its therapeutic potential (analgesic in the context of this study).

CRediT authorship contribution statement

Antonio J. Ortiz: Writing – original draft, Visualization, Methodology, Investigation, Formal analysis, Conceptualization. **Víctor Martín:** Methodology, Investigation, Formal analysis. **David Romero:** Writing – original draft, Supervision, Methodology, Investigation, Formal analysis, Conceptualization. **Antoni Guillamon:** Writing – review & editing, Writing – original draft, Visualization, Supervision, Methodology, Investigation, Formal analysis, Conceptualization. **Jesús Giraldo:** Writing – review & editing, Writing – original draft, Visualization, Supervision, Resources, Project administration, Methodology, Investigation, Funding acquisition, Formal analysis, Conceptualization.

Declaration of competing interest

The authors declare that they have no known competing financial interests or personal relationships that could have appeared to influence the work reported in this paper.

Data availability

Data will be made available on request.

Acknowledgements

This project has received funding from the European Union's Horizon 2020 research and innovation program under grant agreement No 848068. This publication reflects only the authors' view and the European Commission is not responsible for any use that may be made of the information it contains. This work is partially supported by the grants PID2020-119136RB-I00, PID-2021-122954NB-I00, PID2022-137708NB-I00 and the Severo Ochoa and María de Maeztu Programs for Centers and Units of Excellence in R&D (CEX2020-001084-M) funded by MCIN/AEI/10.13039/501100011033 and by ERDF "A way of making Europe", and by the AGAUR grant 2021-SGR-01039. AJO is funded by FPI fellowship (PRE2021-100772) associated to PID2020-119136RB-I00 grant.

Appendix A. Uniqueness and stability of the equilibrium for case 1

We provide the technical details that prove that system (11) has a unique equilibrium point, we give its explicit expression, and we prove, using the Routh-Hurwitz theorem, that this equilibrium point is always stable.

System (11) can be expressed as X' = MX + b, where

$$M := \begin{pmatrix} -[A_{tot}]k_1 - [B_{tot}]k_2 & k_{-1} & k_{-2} \\ [A_{tot}]k_1 - k_{-3} & -k_{-1} - k_{-3} - [B_{tot}]k_3 & -k_{-3} \\ [B_{tot}]k_2 - k_4 & -k_4 & -k_{-4} - k_{-2} - [A_{tot}]k_4 \end{pmatrix},$$

$$b := \begin{pmatrix} 0 \\ k_{-3}[R_{tot}] \\ k_{-4}[R_{tot}] \end{pmatrix}.$$

It is easy to see that the determinant of the system is

$$\begin{aligned}\det(M) = & -[A_{tot}]^2[B_{tot}]k_1k_3k_4 - [A_{tot}][B_{tot}]^2k_2k_3k_4 - [A_{tot}]^2k_1k_4k_{-3} - [A_{tot}][B_{tot}]k_1k_3k_{-4} - [A_{tot}][B_{tot}]k_1k_3k_{-2} - [A_{tot}][B_{tot}]k_2k_4k_{-1} - [A_{tot}][B_{tot}]k_2k_4k_{-3} \\ & - [B_{tot}]^2k_2k_3k_{-4} - [A_{tot}]k_1k_{-2}k_{-3} - [A_{tot}]k_1k_{-2}k_{-4} - [A_{tot}]k_4k_{-1}k_{-3} - [B_{tot}]k_2k_{-1}k_{-3} - [B_{tot}]k_2k_{-1}k_{-4} - [B_{tot}]k_3k_{-2}k_{-4} - k_{-1}k_{-2}k_{-3} - k_{-1}k_{-2}k_{-4}\end{aligned}$$

which is clearly different from zero because all parameters are positive. Then, it has a unique equilibrium point x_0. Tedious but straightforward computations lead to the following expressions for the three components of $x_0 = (x_0^{(1)}, x_0^{(2)}, x_0^{(3)})$:

$$x_0^{(1)} = \frac{N_0^{(1)}}{D_0}$$

where

$$N_0^{(1)} = [R_{tot}](k_{-1}k_4k_{-2} + k_{-1}k_{-2}k_{-3} + [A_{tot}]k_{-1}k_4k_{-3} + [B_{tot}]k_3k_4k_{-2})$$

and

$$\begin{aligned}D_0 = & k_4k_1k_2 + k_1k_2k_3 + [A_{tot}]^2k_1k_4k_3 + [B_{tot}]^2k_2k_3k_4 + [A_{tot}]k_1k_4k_2 + [A_{tot}]k_1k_2k_3 + [A_{tot}]k_4k_1k_3 + [B_{tot}]k_2k_4k_1 + [B_{tot}]k_3k_4k_2 + [B_{tot}]k_2k_1k_3 + [A_{tot}][B_{tot}]k_1k_3k_4 \\ & + [A_{tot}][B_{tot}]k_1k_3k_2 + [A_{tot}][B_{tot}]k_2k_4k_1 + [A_{tot}][B_{tot}]k_2k_4k_3 + [A_{tot}]^2[B_{tot}]k_1k_3k_4 + [A_{tot}][B_{tot}]^2k_2k_3k_4;\end{aligned} \tag{A1}$$

$$x_0^{(2)} = \frac{N_0^{(2)}}{D_0},$$

where

$$N_0^{(2)} = [R_{tot}]\left([A_{tot}]^2k_4k_1k_{-3} + [A_{tot}]k_4k_1k_{-2} + [A_{tot}]k_1k_{-2}k_{-3} + [A_{tot}][B_{tot}]k_2k_4k_{-3}\right); \tag{A2}$$

and

$$x_0^{(3)} = \frac{N_0^{(3)}}{D_0},$$

where

$$N_0^{(3)} = [R_{tot}]\left([B_{tot}]^2k_2k_3k_4 + [B_{tot}]k_{-1}k_2k_{-3} + [B_{tot}]k_{-1}k_2k_4 + [A_{tot}][B_{tot}]k_3k_4k_1\right). \tag{A3}$$

We compute the Jacobian matrix of the system [35] in order to study the local behavior of the equilibrium point x_0. In fact, since the system is linear, the Jacobian matrix is constant and equals M:

$$J(x_0) = M = \begin{pmatrix} -[A_{tot}]k_1 - [B_{tot}]k_2 & k_{-1} & k_{-2} \\ [A_{tot}]k_1 - k_{-3} & -k_{-1} - k_{-3} - [B_{tot}]k_3 & -k_{-3} \\ [B_{tot}]k_2 - k_4 & -k_4 & -k_{-4} - k_{-2} - [A_{tot}]k_4 \end{pmatrix} \tag{A4}$$

To avoid cumbersome notation, we define: $a = [A_{tot}]k_1$, $b = [B_{tot}]k_2$, $c = k_{-1}$, $d = k_{-2}$, $e = k_{-3}$, $f = [B_{tot}]k_3$, $g = k_4$ and $h = [A_{tot}]k_4$. Thus,

$$J(x_0) = \begin{pmatrix} -(a+b) & c & d \\ a-e & -(c+e+f) & -e \\ b-g & -g & -(d+g+h) \end{pmatrix}. \tag{A5}$$

The local stability of the equilibrium point is decided from the eigenvalues (λ), that is, the solutions of the characteristic polynomial $p(\lambda) = \det(J(x_0) -$

λId) = 0, where Id is the 3x3 identity matrix, and det is the determinant. Substituting (A5) in p(λ), we get

$$p(\lambda) = -\lambda^3 + p_1\lambda^2 + p_2\lambda + p_3,$$

being

$$\begin{aligned} p_1 &= -(a+b+c+d+e+f+g+h),\\ p_2 &= -(ad+bc+ae+af+be+cd+ag+bf+ce+ah+bg+de+bh+cg+df+ch+dg+eh+fg+fh),\\ p_3 &= -(ade+bce+adf+adg+bcg+cde+bch+aeh+afg+cdg+afh+beh+bfg+bfh+ceh+dfg). \end{aligned} \tag{A6}$$

We then apply the Routh-Hurwitz Criterion (see, for instance, [38]) to analyze the stability of the equilibrium point. This stability criterion stablishes that the roots of a polynomial have negative real part (which ensures stability) if and only if $p_1 < 0$, $p_2 < 0$, $p_3 < 0$ (which are true because all parameters a, b, c, d, e, f, g, h are positive) and $p_1p_2 > -p_3$ (which is also true for the same reason).

Appendix B. Equilibria and their stability character for a specific example of case 2

The quadratic ODE system (12) has three different equilibrium points, and because of the difficulties of using general formulas in this case, we substitute the parameter values (already used in Fig. 5) into the system. By equating to zero the right-hand side expressions of system (12), we get the following three equilibria:

$$x_0^{(1)} = \left(-2.1617\cdot10^{-8}, 5.6234\cdot10^{-9}, 8.6168\cdot10^{-9}\right), \tag{B1}$$

$$x_0^{(2)} = \left(-9.6873\cdot10^{-12}, 1.0323\cdot10^{-13}, -9.6873\cdot10^{-11}\right), \tag{B2}$$

$$x_0^{(3)} = \left(4.6898\cdot10^{-12}, 2.4194\cdot10^{-14}, 4.4898\cdot10^{-11}\right). \tag{B3}$$

Note that, whereas $x_0^{(3)}$ belongs to the first octant (all coordinates are positive), the other two equilibria have some negative coordinates. Thus, $x_0^{(3)}$ is the only biologically plausible equilibrium. Nevertheless, we classify all of them to get a general picture. We first compute the general Jacobian matrix:

$$J(x_0) = \begin{pmatrix} -k_1([A_{tot}]-[R_{tot}]+2x+z)-[B_{tot}]k_2 & k_{-1} & k_{-2}-k_1x \\ k_1([A_{tot}]-[R_{tot}]+2x+z)-k_{-3} & -k_{-1}-k_{-3}-[B_{tot}]k_3 & -k_{-3}+k_1x \\ [B_{tot}]k_2-k_{-4}-k_4z & -k_4 & -k_{-4}-k_{-2}-k_4([A_{tot}]-[R_{tot}]+x+2z) \end{pmatrix} \tag{B4}$$

After substituting (x,y,z) in (B4) by the values of $x_0^{(1)}$, $x_0^{(2)}$ and $x_0^{(3)}$, we get:

$$J\left(x_0^{(1)}\right) = \begin{pmatrix} 0.2462 & 0.1 & 0.2262 \\ -0.3464 & -0.5002 & -0.2164 \\ -0.0733 & -0.001 & 0.0767 \end{pmatrix} \tag{B5}$$

$$J\left(x_0^{(2)}\right) = \begin{pmatrix} -0.0988 & 0.1 & 0.0101 \\ -0.0014 & -0.5002 & -0.0003 \\ 0.1009 & -0.001 & -0.0069 \end{pmatrix} \tag{B6}$$

$$J\left(x_0^{(3)}\right) = \begin{pmatrix} -0.1006 & 0.1 & 0.01 \\ 0.0004 & -0.5002 & -0.0002 \\ 0.0981 & -0.001 & -0.013 \end{pmatrix} \tag{B7}$$

By solving the characteristic polynomial, we get the eigenvalues (denoted by $\lambda_i^{(j)}$) corresponding to each equilibrium point. For $x_0^{(1)}$, we obtain the approximate values:

$$\begin{cases} \lambda_1^{(1)} = -0.4485, \\ \lambda_2^{(1)} = 0.1356 + 0.1079i, \\ \lambda_3^{(1)} = 0.1356 - 0.1079i. \end{cases} \tag{B8}$$

For $x_0^{(2)}$, the eigenvalues are, approximately:

$$\begin{cases} \lambda_1^{(2)} = -0.1091, \\ \lambda_2^{(2)} = 0.003, \\ \lambda_3^{(2)} = -0.5; \end{cases} \tag{B9}$$

and for $x_0^{(3)}$:

$$\begin{cases} \lambda_1^{(3)} = -0.003, \\ \lambda_2^{(3)} = -0.1104, \\ \lambda_3^{(3)} = -0.5003. \end{cases} \tag{B10}$$

The three equilibrium points are hyperbolic because none of their eigenvalues present zero real part. The first equilibrium point ($x_0^{(1)}$) is a focus-saddle point because it has one real eigenvalue with negative sign and a pair of complex conjugate eigenvalues with positive real part. This type of equilibrium is always unstable. The second equilibrium point ($x_0^{(2)}$) is a saddle point because its three eigenvalues are real but do not have the same sign, and it is also an unstable equilibrium point. The three eigenvalues associated to the third equilibrium point ($x_0^{(3)}$) are real and negative, and consequently, it is a stable node. Therefore, the unique stable equilibrium point is the third one, while the other two are unstable.

Summarizing, equilibria $x_0^{(1)}$ and $x_0^{(2)}$ are not biologically plausible because some of their coordinates are negative (recall that variables x, y and z have to be necessarily positive because they are concentrations). Therefore, $x_0^{(3)}$ is the only biologically significant equilibrium point of the system; moreover, it is stable and so all trajectories with initial conditions close enough to $x_0^{(3)}$ tend to this point as time goes to infinity. In Appendix C, we prove, in addition, that the basin of attraction of $x_0^{(3)}$ (the set of initial conditions whose solutions tend to $x_0^{(3)}$) is large and we give arguments to support that it is indeed the unique attractor for all values of the parameters, thus ruling out also multistationarity.

Appendix C. Existence of a unique biologically plausible equilibrium point

We will base our proof on showing the existence of a so-called *invariant region* in the phase space, that is, the space of the concentrations of the species (for system (12), it is a three-dimensional space). A region Ω is *positively invariant* if all trajectories whose initial condition belongs to Ω remain in Ω for all $t > 0$. A natural way to define this region is by searching for a plane of the form $ax + by + cz = d$ that forms a tetrahedron with the three coordinated planes $x = 0$, $y = 0$ and $z = 0$ (remind that x, y and z are the concentrations of the different heterodimeric species). Since we want this invariant region to be in the first octant, we can assume that a, b, c, $d \geq 0$ without loss of generality. Therefore, we consider the region

$$\Omega_{a,b,c,d} = \{(x,y,z) : ax + by + cz \leq d, x \geq 0, y \geq 0, z \geq 0 \text{ for } a,b,c,d \geq 0\}. \tag{C1}$$

To simplify notation, we drop the subscripts of $\Omega_{a,b,c,d}$ from now on. In order to proof that Ω is a positively invariant region, we need to see that the solutions (x(t), y(t), z(t)) of system (12) point to the interior of Ω when crossing the surfaces $\{x = 0\} \cap \Omega$, $\{y = 0\} \cap \Omega$, $\{z = 0\} \cap \Omega$ and $\{ax + by + cz = d\} \cap \Omega$.

For the three coordinated planes, it is equivalent to see that $x' > 0$, $y' > 0$ and $z' > 0$ when $x = 0$, $y = 0$ and $z = 0$, respectively, in system (4). For instance, for $x = 0$, we have that $x' = k_{-1}y + k_{-2}z$ which is clearly positive on $\{x = 0\} \cap \Omega$. In a similar way, we can check that it also happens with y' and z'.

In order to see that the solutions point to the interior of Ω for the non-coordinate plane $ax + by + cz = d$, we need to prove that

$$(x', y', z') \cdot (a, b, c) < 0 \text{ for } x, y, z \geq 0 \tag{C2}$$

where the dot between the two vectors stands for the scalar product.

We are going to prove this property for (a,b,c) = (1,1,1) (other choices could work as well) and let d be free. Direct computations give

$$(x', y', z') \cdot (1,1,1) = -(k_{-3} + k_{-4})(d - [R_{tot}]) - k_4[A]z - k_3[B]y \tag{C3}$$

Observe that all terms in this expression are negative whenever $d \geq [R_{tot}]$. Thus, the desired property follows under this condition and we can assert that any region

$$\Omega_d = \{(x,y,z) : x + y + z \leq d, x \geq 0, y \geq 0, z \geq 0, d \geq [R_{tot}]\} \tag{C4}$$

is positively invariant. Fig. C1 shows a typical tetrahedral region Ω_d together with the equilibrium point.

References

[1] E. Akgün, M.I. Javed, M.M. Lunzer, B.A. Smeester, A.J. Beitz, P.S. Portoghese, Ligands that interact with putative MOR-mGluR5 heteromer in mice with inflammatory pain produce potent antinociception, Proc. Natl. Acad. Sci. 110 (28) (2013) 11595–11599, https://doi.org/10.1073/pnas.1305461110.

[2] R.J. Bodnar, Endogenous opiates and behavior: 2021, Peptides 164 (2023) 171004, https://doi.org/10.1016/j.peptides.2023.171004.

[3] D.O. Borroto-Escuela, K. Fuxe, Oligomeric Receptor Complexes and Their Allosteric Receptor-Receptor Interactions in the Plasma Membrane Represent a New Biological Principle for Integration of Signals in the CNS, Front. Mol. Neurosci. 12 (2019), https://doi.org/10.3389/fnmol.2019.00230.

[4] M. Bouvier, T.E. Hébert, CrossTalk proposal: Weighing the evidence for Class A GPCR dimers, the evidence favours dimers, J. Physiol. 592 (12) (2014) 2439–2441, https://doi.org/10.1113/jphysiol.2014.272252.

[5] N.C. Dale, E.K.M. Johnstone, K.D.G. Pfleger, GPCR heteromers: An overview of their classification, function and physiological relevance, Front. Endocrinol. 13 (2022), https://doi.org/10.3389/fendo.2022.931573.

[6] D.J. Daniels, N.R. Lenard, C.L. Etienne, P.-Y. Law, S.C. Roerig, P.S. Portoghese, Opioid-induced tolerance and dependence in mice is modulated by the distance between pharmacophores in a bivalent ligand series, Proc. Natl. Acad. Sci. 102 (52) (2005) 19208–19213, https://doi.org/10.1073/pnas.0506627102.

[7] Ó. Díaz, V. Martín, P. Renault, D. Romero, A. Guillamon, J. Giraldo, Allosteric binding cooperativity in a kinetic context, Drug Discov. Today d(2) (2022) 103441, https://doi.org/10.1016/j.drudis.2022.103441.

[8] M. Feinberg, Foundations of Chemical Reaction Network Theory. Applied Mathematical Sciences, (1st ed.)., Springer, Cham, 2019.

[9] S. Ferré, R. Franco, Oligomerization of G-protein-coupled receptors: A reality, Curr. Opin. Pharmacol. 10 (1) (2010) 1–5, https://doi.org/10.1016/j.coph.2009.11.002.

[10] M. Fribourg, J.L. Moreno, T. Holloway, D. Provasi, L. Baki, R. Mahajan, G. Park, S. K. Adney, C. Hatcher, J.M. Eltit, J.D. Ruta, L. Albizu, Z. Li, A. Umali, J. Shim, A. Fabiato, A.D. MacKerell, V. Brezina, S.C. Sealfon, D.E. Logothetis, Decoding the Signaling of a GPCR Heteromeric Complex Reveals a Unifying Mechanism of Action of Antipsychotic Drugs, Cell 147 (5) (2011) 1011–1023, https://doi.org/10.1016/j.cell.2011.09.055.

[11] W. Fujita, I. Gomes, L.A. Devi, Revolution in GPCR signalling: opioid receptor heteromers as novel therapeutic targets: IUPHAR Review 10, Br. J. Pharmacol. 171 (18) (2014) 4155–4176, https://doi.org/10.1111/bph.12798.

[12] T. Galvez, Allosteric interactions between GB1 andGB2 subunits are required for optimalGABAB receptor function, EMBO J. 20 (9) (2001) 2152–2159, https://doi.org/10.1093/emboj/20.9.2152.

[13] I. Gilron, T.S. Jensen, A.H. Dickenson, Combination pharmacotherapy for management of chronic pain: from bench to bedside, The Lancet Neurology 12 (11) (2013) 1084–1095, https://doi.org/10.1016/S1474-4422(13)70193-5.
[14] J. Giraldo, B. Zhou, D. Roche, C. Gil, J. Ortiz, I. Lans, J. Dalton, P. Renault, Analysis of the Function of Receptor Oligomers by Operational Models of Agonism, in: Comprehensive Pharmacology, Elsevier, 2022, pp. 337–359, https://doi.org/10.1016/B978-0-12-820472-6.00012-8.
[15] I. Gomes, M.A. Ayoub, W. Fujita, W.C. Jaeger, K.D.G. Pfleger, L.A. Devi, G Protein-Coupled Receptor Heteromers, Annu. Rev. Pharmacol. Toxicol. 56 (1) (2016) 403–425, https://doi.org/10.1146/annurev-pharmtox-011613-135952.
[16] D. Guo, L.A. Peletier, L. Bridge, W. Keur, H. de Vries, A. Zweemer, L.H. Heitman, A. P. IJzerman, A two-state model for the kinetics of competitive radioligand binding, Br. J. Pharmacol. 175 (10) (2018) 1719–1730, https://doi.org/10.1111/bph.14184.
[17] V.V. Gurevich, E.V. Gurevich, GPCRs and Signal Transducers: Interaction Stoichiometry, Trends Pharmacol. Sci. 39 (7) (2018) 672–684, https://doi.org/10.1016/j.tips.2018.04.002.
[18] S.J. Hill, L.E. Kilpatrick, Kinetic analysis of fluorescent ligand binding to cell surface receptors: Insights into conformational changes and allosterism in living cells, Br. J. Pharmacol. (2023), https://doi.org/10.1111/bph.16185.
[19] S.R.J. Hoare, P.H. Tewson, A.M. Quinn, T.E. Hughes, L.J. Bridge, Analyzing kinetic signaling data for G-protein-coupled receptors, Sci. Rep. 10 (1) (2020) 12263, https://doi.org/10.1038/s41598-020-67844-3.
[20] H. Hübner, T. Schellhorn, M. Gienger, C. Schaab, J. Kaindl, L. Leeb, T. Clark, D. Möller, P. Gmeiner, Structure-guided development of heterodimer-selective GPCR ligands, Nat. Commun. 7 (1) (2016) 12298, https://doi.org/10.1038/ncomms12298.
[21] IJzerman, A. P., & Guo, D. (2019). Drug–Target Association Kinetics in Drug Discovery. *Trends in Biochemical Sciences*, *44*(10), 861–871. doi: 10.1016/j.tibs.2019.04.004.
[22] R. Iyengar, Complex diseases require complex therapies, EMBO Rep. 14 (12) (2013) 1039–1042, https://doi.org/10.1038/embor.2013.177.
[23] N.A. Lambert, J.A. Javitch, CrossTalk opposing view: Weighing the evidence for class A GPCR dimers, the jury is still out, J. Physiol. 592 (12) (2014) 2443–2445, https://doi.org/10.1113/jphysiol.2014.272997.
[24] M. Le Naour, E. Akgün, A. Yekkirala, M.M. Lunzer, M.D. Powers, A.E. Kalyuzhny, P.S. Portoghese, Bivalent Ligands That Target μ Opioid (MOP) and Cannabinoid1 (CB 1) Receptors Are Potent Analgesics Devoid of Tolerance, J. Med. Chem. 56 (13) (2013) 5505–5513, https://doi.org/10.1021/jm4005219.
[25] J. Levitz, C. Habrian, S. Bharill, Z. Fu, R. Vafabakhsh, E.Y. Isacoff, Mechanism of Assembly and Cooperativity of Homomeric and Heteromeric Metabotropic Glutamate Receptors, Neuron 92 (1) (2016) 143–159, https://doi.org/10.1016/j.neuron.2016.08.036.
[26] H.-C. Lu, K. Mackie, Review of the Endocannabinoid System, Biological Psychiatry: Cognitive Neuroscience and Neuroimaging 6 (6) (2021) 607–615, https://doi.org/10.1016/j.bpsc.2020.07.016.
[27] Martín, V. (2022). Modelization and study of the heterodimerization process of G Protein-Coupled Receptors: towards combined drug therapies (Master's Thesis) [Universitat Politècnica de Catalunya]. https://upcommons.upc.edu/handle/2117/375019.
[28] J. Meng, C. Xu, P.-A. Lafon, S. Roux, M. Mathieu, R. Zhou, P. Scholler, E. Blanc, J.A. J. Becker, J. Le Merrer, J. González-Maeso, P. Chames, J. Liu, J.-P. Pin, P. Rondard, Nanobody-based sensors reveal a high proportion of mGlu heterodimers in the brain, Nat. Chem. Biol. 18 (8) (2022) 894–903, https://doi.org/10.1038/s41589-022-01050-2.
[29] D. Moreno Delgado, T.C. Møller, J. Ster, J. Giraldo, D. Maurel, X. Rovira, P. Scholler, J.M. Zwier, J. Perroy, T. Durroux, E. Trinquet, L. Prezeau, P. Rondard, J.-P. Pin, Pharmacological evidence for a metabotropic glutamate receptor heterodimer in neuronal cells, Elife 6 (2017), https://doi.org/10.7554/eLife.25233.
[30] P.S. Portoghese, E. Akgün, M.M. Lunzer, Heteromer Induction: An Approach to Unique Pharmacology? ACS Chem. Nerosci. 8 (3) (2017) 426–428, https://doi.org/10.1021/acschemneuro.7b00002.
[31] L. Prezeau, M.-L. Rives, L. Comps-Agrar, D. Maurel, J. Kniazeff, J.-P. Pin, Functional crosstalk between GPCRs: with or without oligomerization, Curr. Opin. Pharmacol. 10 (1) (2010) 6–13, https://doi.org/10.1016/j.coph.2009.10.009.
[32] M. Qian, Z. Sun, X. Chen, S. Van Calenbergh, Study of G protein-coupled receptors dimerization: From bivalent ligands to drug-like small molecules, Bioorg. Chem. 140 (2023) 106809, https://doi.org/10.1016/j.bioorg.2023.106809.
[33] X. Rovira, J.-P. Pin, J. Giraldo, The asymmetric/symmetric activation of GPCR dimers as a possible mechanistic rationale for multiple signalling pathways, Trends in Pharmacological Sciences 31 (1) (2010) 15–21, https://doi.org/10.1016/j.tips.2009.10.008.
[34] S. Saha, J. González-Maeso, The crosstalk between 5-HT2AR and mGluR2 in schizophrenia, Neuropharmacology 230 (2023) 109489, https://doi.org/10.1016/j.neuropharm.2023.109489.
[35] G. Strang, Differential Equations and Linear Algebra, Wellesley-Cambridge Press, 2015.
[36] D.A. Sykes, L.A. Stoddart, L.E. Kilpatrick, S.J. Hill, Binding kinetics of ligands acting at GPCRs, Mol. Cell. Endocrinol. 485 (2019) 9–19, https://doi.org/10.1016/j.mce.2019.01.018.
[37] C. White, L.J. Bridge, Ligand Binding Dynamics for Pre-dimerised G Protein-Coupled Receptor Homodimers: Linear Models and Analytical Solutions, Bull. Math. Biol. 81 (9) (2019) 3542–3574, https://doi.org/10.1007/s11538-017-0387-x.
[38] S. Wiggins, in: Introduction to Applied Nonlinear Dynamical Systems and Chaos, Springer-Verlag, 2003, https://doi.org/10.1007/b97481.
[39] H. Xu, L. Staszewski, H. Tang, E. Adler, M. Zoller, X. Li, Different functional roles of T1R subunits in the heteromeric taste receptors, Proc. Natl. Acad. Sci. 101 (39) (2004) 14258–14263, https://doi.org/10.1073/pnas.0404384101.
[40] B. Zhou, J. Giraldo, Quantifying the allosteric interactions within a G-protein-coupled receptor heterodimer, Drug Discov. Today 23 (1) (2018) 7–11, https://doi.org/10.1016/j.drudis.2017.07.009.